Supplementary material: Alternative dissipation mechanisms and the effect of the solvent in friction between polymer brushes on rough surfaces

Sissi de Beer and Martin H. Müser

May 4, 2013

We use a generic Lennard Jones (LJ) model (with σ and ϵ the characteristic length-scale and energy respectively). Unless explicitly stated differently in the main text, our system consists of a symmetric contact between two curved surfaces (radius $R = 100\sigma$) both bearing 3828 polymer chains (degree of polymerization $N = 30$) with a grafting density $\alpha_g = 0.16\sigma^{-2}$. The polymers are solvated using dimers. Their rotational degrees of freedom will reduce artificial effects due to layering at the walls compared to single monomers[1]. The walls are crystalline surfaces (fcc [111]) with a lattice constant of 1.2σ. The wall atoms are connected to their lattice sites with harmonic springs ($k = 32\epsilon/\sigma^2$) and to each other using an anharmonic spring ($k = 30\epsilon/\sigma^2$) ensuring a maximum

displacement of 0.4 σ. To translate the surfaces with respect to each other, we move the lattice sites of both surfaces symmetrically in opposite directions with a constant velocity. Periodic boundary conditions are applied in x and y.

The monomers of the grafted polymers interact via the Kremer-Grest (KG) model[2], where the LJ interaction between consecutive monomers is purely repulsive ($\epsilon = 1$, $\sigma = 1$ and $r_{cut} = 2^{1/6}\sigma$) and the connection is assured via the FENE potential using a stiffness $k = 30\epsilon/\sigma^2$ and a maximum extension $R_o = 1.5\sigma$. For the dimers we use the same potential with a maximum extension of $R_o = 1.3\sigma$ to create a size mismatch that will further reduce layering. The LJ parameters are adjusted to $\epsilon = 0.8$, $\sigma = 0.8$ such that the potential for both the dimers and the polymers is equally shaped. The polymers are connected to the walls with a similar shape-matched KG model ($\epsilon = 0.8$, $\sigma = 1.5$, $k = 30\epsilon/\sigma^2$ and $R_o = 2.1\sigma$). Non-consecutive monomers of the polymers interact via the LJ potential using the same ϵ and σ as consecutive monomers, but with a cut-off of 1.6 σ, making the polymers slightly attractive. Between non-connected dimer-monomers we chose our parameters to be $\epsilon = 0.5$, $\sigma = 1$ and $r_{\text{cut}} = 2.5\sigma$, which keeps the dimers in the liquid phase over the entire range of pressures used in the simulations ($P = 0 - 25\epsilon/\sigma^3$). The LJ parameters for the interaction between dimer and polymer are $\epsilon = 1.2$, $\sigma = 1$ and $r_{cut} = 2.5\sigma$. Due to our choice for the LJ parameters we have good solvent conditions[3]. Our brushes are undersaturated with solvent (we used half the amount of solvent needed to saturate the brushes) and therefore in a more collapsed state than saturated brushes. For the interactions of the brush and of the solvent with

the walls we chose a larger σ to keep all the liquid-particles between the walls ($\epsilon = 0.6$, $\sigma = 1.3$ and $r_{cut} = 1.6\sigma$).

The equations of motions for all mobile particles are solved using the velocity Verlet algorithm as implemented in LAMMPS[4] using a time-step of $\Delta t = 0.005\sigma \left(m/\epsilon\right)^{0.5}$ (a time step of $0.001 \ \sigma \left(m/\epsilon\right)^{0.5}$ does not change our results). The temperature in the simulation box is kept constant at $T = 0.6\epsilon/k_B$ using a Langevin thermostat applied perpendicular to the direction of motion on the wall-atoms alone, to guarantee no interference of the thermostat with the (hydro-)dynamics of the system. For the thermostat we chose a time-constant of $\tau = 1\sigma \left(m/\epsilon\right)^{0.5}$.

We averaged the forces in y over 2-3 periodic images for each velocity. The forces in x were averaged over at least 1 periodic images. For the lowest velocity ($v = 4 \cdot 10^{-5}\sigma/\tau$, which translates to < 1 cm/s in real time) we required $3 \cdot 10^8$ timesteps, corresponding to 500,000 core-hours using 2048 cores. In total, we needed 10 million core-hours on a Blue Gene P system (Jugene, FZ Jülich) for the non-equilibrium simulations and 50,000 core-hours on an Intel Xeon X5570 (Nehalem-EP) based supercomputer (Juropa, FZ Jülich) for the equilibrium simulations.
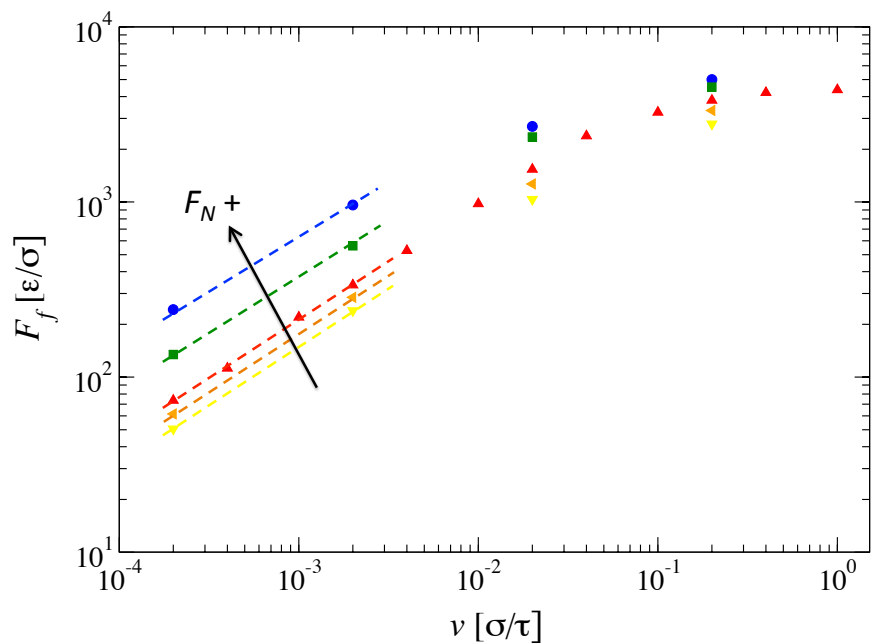
Figure 1: The friction force F_f versus velocity for different normal pressures between -30 and 400 MPa. The effective exponent was found to be $\kappa = 0.67 \pm 0.02$.

In the main text we claim that for motion in x at low velocities the effective shear-thinning exponent is independent of the applied normal load (or the distance between the cylinders). This is supported by ESI Fig. 1, which shows the friction force for motion in x for different distances d between the cylinders apex (blue circles $d = 8\sigma$, green squares $d = 10\sigma$, ... , yellow downward triangles $d = 18\sigma$). Despite the fact that the data was fitted using only two datapoint per normal load, we find a constant effective exponent of $\kappa = 0.67 \pm 0.02$.
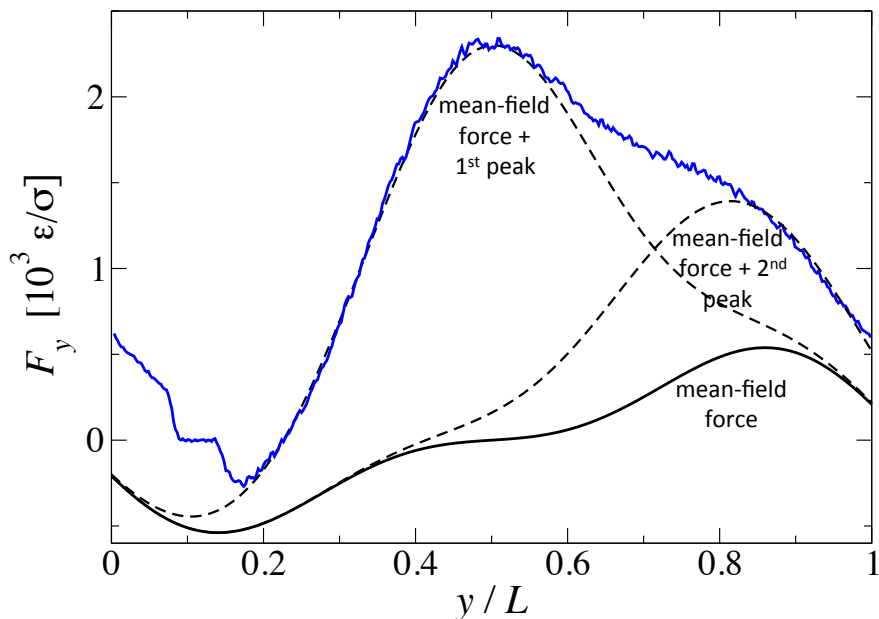
4

Figure 2: Identification and fitting of the two peaks in the force traces upon asperity collision.

In the main text we discuss that for the force-traces for motion in y we fitted the first peak and the shoulder (which turns into a second peak after subtraction of the first peak) using a Gaussian function. This is shown in ESI Fig. 2. The black line denotes the mean-field force, which was determined by equilibrating the system at different position for y/L. The dashed lines denote the meanfield force + the fitted Gaussian peaks. The first peak is symmetric around symmetry-point $y/L = 0.5$, this peak is purely dissipative. The second peak is not symmetric around $y/L = 0.5$ and can thus be decomposed into a symmetric (= dissipative) part and an antisymmetric (= non-dissipative) part.
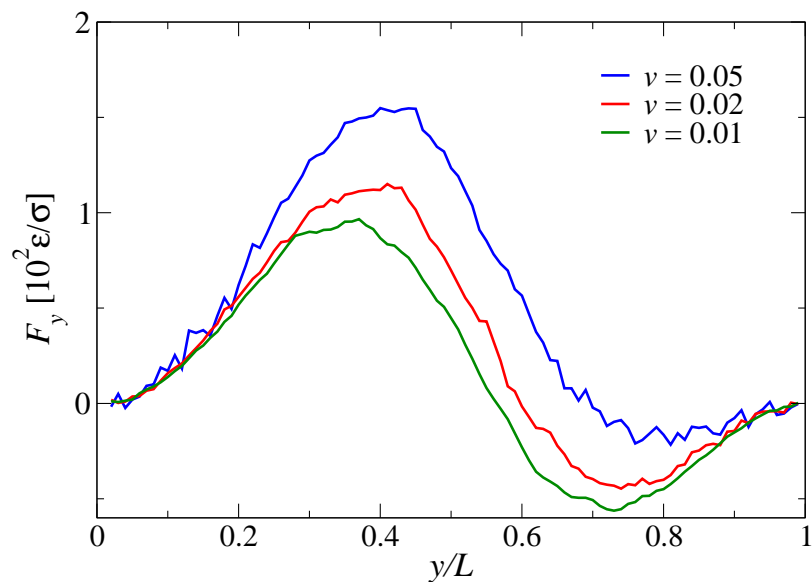
5

Figure 3: The force traces for complete immersion in solvent (no capillary due to the surface tension of the solvent).

In the main text we claim that the force-traces for motion in y become qualitatively different when the contact is completely immersed in solvent. This is shown in ESI Fig. 3. Upon complete immersion in solvent the capillary due to the surface tension of the solvent disappears and the second peak is no longer visible in the force-traces. This implies that a capillary due to surface tension strongly enhances transient effects[5].
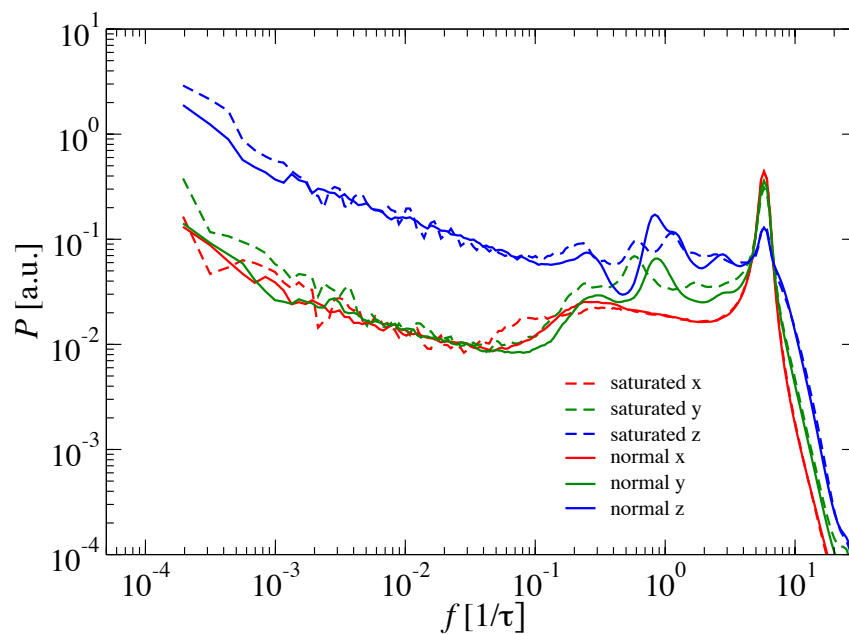
Figure 4: The powerspectra of our default system compared to the spectra of a fully saturated system (dashed lines).

In the main text we discuss that increasing the amount of solvent to full saturation only slightly affects the spectral response at high frequencies and does not affect the spectral response for low frequencies. This claim is supported by ESI Fig. 4 that shows the spectral response for our default system compared to a fully saturated system (dashed lines).
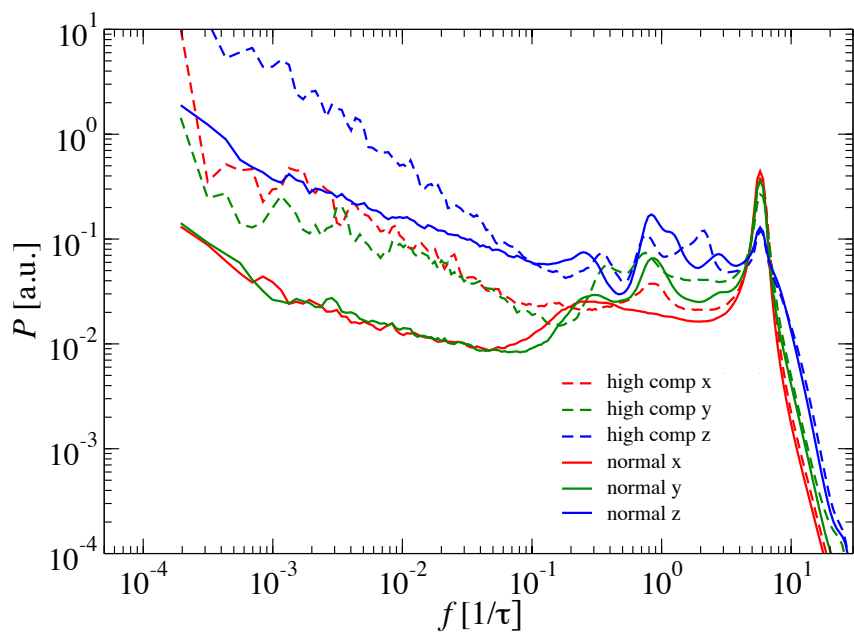
Figure 5: The powerspectra of our default system compared to the spectra of a compressed system (dashed lines).

In the main text we discuss the effect of the normal load on the spectral repsonse of the system. This is shown in more detail in ESI Fig. 5. Upon increasing the normal load the exponent μ at low frequencies alters differently for the different direction x, y and z.

References

[1] A. Galuschko, L. Spirin, T. Kreer, A. Johner, C. Pastorino, J. Wittmer and J. Baschnagel, *Langmuir*, 2010, **26**, 6418.

[2] K. Kremer and G. S. Grest, *J. Chem. Phys.*, 1990, **92**, 5057.

[3] K. Binder, T. Kreer and A. Milchev, *Soft Matter*, 2011, **7**, 7159.

[4] S. Plimpton, *J. Comp. Phys.*, 1995, **117**, 1.

[5] W. J. Briels, *Soft Matter*, 2009, **5**, 4401.